Development of a rapid viability RT-PCR (RV-RT-PCR) method to detect infectious SARS-CoV-2 from swabs

Sanjiv R. Shah [a],[*], Staci R. Kane [b], Maher Elsheikh [b], Teneile M. Alfaro [b]

[a] *Homeland Security and Materials Management Division, Center for Environmental Solutions and Emergency Response, Office of Research and Development, U.S. Environmental Protection Agency, Washington, DC, USA*
[b] *Lawrence Livermore National Laboratory, Livermore, CA, USA*

A B S T R A C T

Since the rapid onset of the COVID-19 pandemic, its causative virus, Severe Acute Respiratory Syndrome Coronavirus-2 (SARS-CoV-2), continues to spread and increase the number of fatalities. To expedite studies on understanding potential surface transmission of the virus and to aid environmental epidemiological investigations, we developed a rapid viability reverse transcriptase PCR (RV-RT-PCR) method that detects viable (infectious) SARS-CoV-2 from swab samples in <1 day compared to several days required by current gold-standard cell-culture-based methods. The method integrates cell-culture-based viral enrichment in a 96-well plate format with gene-specific RT-PCR-based analysis before and after sample incubation to determine the cycle threshold (C_T) difference (ΔC_T). An algorithm based on $\Delta C_T \geq 6$ representing $\sim$ 2-log or more increase in SARS-CoV-2 RNA following enrichment determines the presence of infectious virus. The RV-RT-PCR method with 2-hr viral infection and 9-hr post-infection incubation periods includes ultrafiltration to concentrate virions, resulting in detection of <50 SARS-CoV-2 virions in swab samples in 17 h (for a batch of 12 swabs), compared to days typically required by the cell-culture-based method. The SARS-CoV-2 RV-RT-PCR method may also be useful in clinical sample analysis and antiviral drug testing, and could serve as a model for developing rapid methods for other viruses of concern.

1. Introduction

The ongoing pandemic caused by the Severe Acute Respiratory Syndrome Coronavirus-2 (SARS-CoV-2) continues to consume many lives worldwide, and leaves severe health effects in many recovered patients. According to the U.S. Centers for Disease Control and Prevention (CDC), the principal transmission modes for respiratory viruses such as SARS-CoV-2 are contact, droplet, and airborne (CDC, 2021a,b). Per CDC, contact transmission is infection spread through direct contact with an infectious person or with a contaminated article or surface. Although transmission of SARS-CoV-2 via surfaces is not thought to be the primary way the virus spreads, one may get infected by touching the virus-contaminated surface and then touching one's own mouth, nose, or eyes (CDC, 2021a,b). Surfaces can get contaminated via direct contact or by transmitted respiratory droplets from infected persons. SARS-CoV-2 can be shed not only by symptomatic individuals but also by pre-symptomatic infected individuals, asymptomatic carriers, and

convalescent COVID-19 patients (DeBiasi and Delaney, 2021; Li et al., 2020a,b; Arons et al., 2020; Avanzato et al., 2020; Wei et al., 2020; He et al., 2020; van Kampen et al., 2021; Ferretti et al., 2020; Li et al., 2020a,b; Kampf et al., 2020). The environment and surfaces surrounding such virus carriers can get contaminated by droplets (coughs, sneezes, and other exhalations) and/or surface contact in healthcare and non-healthcare settings (Li et al., 2020a,b; Kampf et al., 2020; Santarpia et al., 2020; Chia et al., 2020; Guo et al., 2020; Ong et al., 2020; Wu et al., 2020; Ye et al., 2020; Luo et al., 2020; Harvey et al., 2021).

Surface contamination, stability of SARS-CoV-2 on different surfaces, and potential indirect transmission of the virus via surfaces have been extensively discussed in several reviews (Kampf et al., 2020; Marquès and Domingo, 2021; Bueckert et al., 2020; Bedrosian et al., 2020; Meyerowitz et al., 2021; Aboubakr et al., 2020). However, more than a year after the emergence of the COVID-19 pandemic, surface transmission of SARS-CoV-2 is still not well understood, and its overall importance in transmission is mostly unknown. Depending on the

material, type of surface, and environmental conditions used in experimental studies, surface stability of SARS-CoV-2 virus was reported from a few hours to days and even up to 28 days for some conditions (Riddell et al., 2020). A majority of the studies for SARS-CoV-2 stability on surfaces have been conducted using the reverse transcriptase polymerase chain reaction (RT-PCR) analytical method to detect viral RNA. The RT-PCR does not distinguish between active (and potentially infectious) and inactive (noninfectious) virus presence, and therefore, SARS-CoV-2 RNA detected from surface samples could also be from inactive virus. Only a limited number of studies used a cell-culture-based method that could detect infectious SARS-CoV-2 on surfaces (Riddell et al., 2020; van Doremalen et al., 2020; Pastorino et al., 2020; Biryukov et al., 2020; Ben-Shmuel et al., 2020). Traditional viral viability methods rely on determination of cytopathic effects (CPE) that occur in host cells when viruses replicate, and use 50% tissue culture infective dose (TCID50) calculations from multiple dilutions of the sample. Though this method is considered a gold standard, it is laborious, and it takes several days to get analytical results due to the long incubation times necessary for observing CPE (Riddell et al., 2020; van Doremalen et al., 2020; Pastorino et al., 2020; Biryukov et al., 2020; Ben-Shmuel et al., 2020). There are potential limitations with these methods to detect infectious virus in environmental samples, where CPE: (i) could be caused by cytotoxic, non-viral constituents in environmental samples (Ridinger et al., 1982); (ii) is subjective and may not be as clear as desired (Agol et al., 1998); and (iii) can be caused by other viruses present in the sample that can infect the cultured cells, thus interfering with detection of the target virus (Schmidt et al., 1978). Limitations of current methods can make it difficult to quickly assess the SARS-CoV-2 survival period on real-world environmental surfaces and to understand surface transmission. This, in turn, seriously impacts environmental epidemiology investigations and transmission studies, where timely knowledge of the presence of infectious virus on a surface is critical. Therefore, a rapid, dependable, and accurate analytical method for detecting infectious SARS-CoV-2 in environmental surface samples (e.g., swabs) is needed. The ability to rapidly detect infectious SARS-CoV-2 would also be valuable for epidemiology investigations and environmental surveillance in healthcare and other facilities (e.g., prisons, nursing homes), and within communities. Here, we report development of a Rapid Viability-Reverse Transcriptase PCR (RV-RT-PCR) method for detection of infectious SARS-CoV-2 in hours, rather than several days typical of the currently used cell-culture-based methods.

The SARS-CoV-2 RV-RT-PCR method followed the principle of rapid viability-PCR (RV-PCR) methods for detection of high-priority bacterial biothreat agents in environmental samples (Létant et al., 2011; Kane et al., 2019a,b). Briefly, the RV-RT-PCR method integrates cell-culture-based enrichment of the virus in a sample with virus-gene-specific RT-PCR-based molecular analysis. The integrated cell culture-PCR (ICC-PCR) methods developed for other viruses also combined virus enrichment in cell-culture with PCR (Reynolds et al., 2001; Gallagher and Margolin, 2007; Rigotto et al., 2010), although PCR/RT-PCR was only performed at the end of enrichment. The RV-RT-PCR method requires RT-PCR analysis before and after the cell-culture-virus (sample) incubation and uses a defined algorithm—the resultant cycle threshold (C_T) difference (ΔC_T) between before and after cell-culture-virus incubation RT-PCR analyses—to determine the presence of infectious virus in the sample. A cell-culture-based enrichment of SARS-CoV-2 combined with RT-PCR has been reported to detect infectious virus after 7 days post-infection (Zhou et al., 2020); however, the RV-RT-PCR method, which uses a shorter post-infection incubation period, will allow detection of infectious virus in hours rather than days.

2. Materials and methods

2.1. Cell culture conditions

The Vero E6 cell line (African green monkey kidney cells; ATCC® CRL-1586™, ATCC; Manassas, VA) was selected for propagation of the SARS-CoV-2 virus. The Vero E6 cells were grown and maintained in Dulbecco's Modified Eagle's Medium (DMEM) (VWR, Radnor, PA; Cat. No. 95042-512) with Fetal Bovine Serum (FBS; Gibco; Life Technologies, Grand Island, NY; Cat. No. 10082-147) and 1X Pen/Strep/Fungizone (100X, VWR; Cat. No. 12001-712) in T-75 flasks (75 cm^2; VWR; Cat. No. 75875-050). The growth medium contained 10% FBS while the maintenance medium contained 2% FBS. The cell culture media contained 1X Pen/Strep/Fungizone for all applications, although this is often abbreviated as 2% FBS DMEM or 10% FBS DMEM.

The Vero E6 cell line was maintained by passaging approximately twice a week. The cells sub-culture procedure involved removing the outgrowth medium and washing the cells with 5 mL Phosphate Buffered Saline (PBS; VWR; Cat. No. 97062-818). Then, 0.5 mL trypsin (VWR; Cat. No. MSPP-30-2101) was added and incubated for 3−7 min at 37°C in 5% CO_2. Trypsin was then neutralized by adding 5 mL 10% FBS DMEM, using a 5-mL or 10-mL serological pipette to pipet the medium up and down to dislodge the cells prior to transferring cells to a 50-mL conical tube, followed by rigorous vortex-mixing to break up cell clumps.

The number of cells needed for virus titration (by TCID50) was 20,000 per well in a 96-well plate (TC-treated; VWR; Cat. No. 10062-900), determined using a Millipore Scepter handheld cell counter (Millipore, Billerica, MA; Cat. No. PHCC20040). For RV-RT-PCR experiments, the cell count was 35,000 cells per well. The cell density was adjusted by adding fresh outgrowth medium. Lower cell densities were used for virus titration (during several days of incubation) to prevent overgrowth and inability to accurately determine viral infection (by CPE). Vero E6 cells required agitation (rocking) while cells were settling onto 96-well plates to prevent clumping. After viral infection, cells were cultured in 2% FBS DMEM and incubated at 37°C in 5% CO_2.

2.2. Preparation of SARS-CoV-2 Stocks

Two or more T-75 flasks (75 cm^2) were seeded by adding $\sim 1 \times 10^6$ Vero E6 in 15−20 mL DMEM with 10% FBS and 1X Pen/Strep/Fungizone. When cells were about 80% confluent (after 1–2 day incubation at 37°C in 5% CO_2), the medium was removed from flasks. Then, 0.5 mL of a -80°C stock of SARS-CoV-2 Isolate USA-WA1/2020 (BEI Resources, Inc., Manassas, VA; Cat. No. NR-52281) was used to infect each flask. The virus was spread across the entire cell monolayer by rocking and swirling the flask by hand. The flasks were incubated for 15 min at 37°C with 5% CO_2 to allow the virus to be absorbed by the cells. Then, 15−20 mL 2% FBS DMEM was added and the flasks were incubated at 37°C with 5% CO_2, and checked daily for CPE using an inverted microscope. When at least 75% of the cells were showing CPE, the virus was harvested by freezing the flasks at -80°C for 10 min, and then thawing the flasks. The flasks were then rigorously shaken from side-to-side to dislodge the monolayer and disperse the host cells. The freezing/thawing/shaking process was repeated three times to lyse the cells and release the virions. Then, the contents of the flasks were removed using serological pipettes and pooled into one or more 50-mL conical tubes. The tube(s) were centrifuged at 3,000–5,000 rpm at 4°C for 3−5 min to pellet cellular debris, and the supernatant was transferred to a new 50-mL conical tube. The tube was vortex-mixed and 0.5-mL aliquots were transferred into labeled cryovials for storage at -80°C.

2.3. Median tissue culture infectious dose (TCID50) analysis

Cell culture preparation for TCID50 analysis included seeding approx. 20,000 cells in each well of a 96-well plate prior to an

experiment using viral infection. When cells were above 90% confluent, 10-fold dilution series of a viral stock were prepared in DMEM with 2% FBS. Twelve wells were infected with 0.1-mL of the viral suspension dilution in a 96-well plate containing cell culture for TCID50 analysis of the viral stock, while quadruplicate wells were used for recovered viral ultrafiltration (UF)-retentates from replicate swabs or swab swatches (0.1 mL/well) (Sections 2.6 and 2.7). In addition, a 0.1-mL aliquot of maintenance medium was also added to each well since the viral UF-retentate was in PBS. Each plate contained four negative wells, which were not infected. The plate with lid was incubated at 37℃ with 5% CO_2 with humidified conditions for up to 10 days, and CPE was monitored using an inverted microscope every 1–2 days. The TCID50 titer (TCID50/mL) was calculated based on the Reed and Muench method (Reed and Muench, 1938).

Data are expressed as TCID50 per 0.1-mL, since 0.1-mL was used to infect cell culture wells. TCID50 analysis was conducted for every experiment to estimate the starting viral concentration. TCID50 values for stock titers are reported as the average and standard deviation in a table footnote for each experiment. This analysis was also used to determine viral recovery efficiency after processing spiked swabs and swatches, with TCID50 results included in a table footnote, as described below. Viral recovery efficiency was either determined from replicate swabs/swatches or from an aliquot of the same viral UF-retentate used for RV-RT-PCR analysis, as specified for each experiment (Section 3 Results and Discussion). The titer expressed as plaque forming units (PFU)/0.1 mL is based on the relationship, $PFU = 0.7 \times TCID50$ (Leibowitz et al., 2011). The standard deviation for the TCID50/0.1 mL and PFU/0.1 mL values were expressed in the table footnote for the appropriate data, as a range above and below the TCID50 or PFU per 0.1/mL, based on the Spearman and Karber algorithm (Hierholzer and Killington, 1996).

2.4. Rapid viability - reverse transcriptase - PCR method

Applying the principle of RV-PCR methods developed for bacterial biothreat agents (Létant et al., 2011; Kane et al., 2019a,b), the SARS-CoV-2 RV-RT-PCR method integrates cell-culture-based enrichment of the virus in a sample with virus-gene-specific RT-PCR-based molecular analysis. The RT-PCR analysis of SARS-CoV-2 RNA is conducted on the same sample both before (time zero or T_0) and after (time final or T_f) the enrichment of the virus in cell-culture to determine the cycle threshold difference (ΔC_T). Both T_0 and T_f represent time in hours. T_0 represents the (experimentally determined) starting time after viral infection (i.e., 1- or 2-hr). T_f represents the endpoint after post-infection incubation (i.e., 9–24 h for method development), also simply referred to as incubation. The sample is split into two equal aliquots for T_0 and T_f, with each added to a well (with adhered cell monolayer) on separate

96-well plates. After the infection period, viral suspensions are removed and the cell culture is washed with 0.1 mL of maintenance medium, after removing the wash media, 0.1 mL of fresh maintenance medium is added. The removal of viral suspension from T_0 and T_f wells after the infection period ensures unattached virions are removed and do not contribute RNA to the background RT-PCR response, thus, resulting in the same initial condition for the sample T_0 and T_f wells. The T_0 well/plate is then processed immediately for RNA extraction (Sections 2.5–2.8) and RT-PCR analysis (Section 2.9), whereas, remaining time-point wells/plates are incubated at 37℃ with 5% CO_2 to the desired endpoint, and then processed as for the T_0 plate. From the T_0 and T_f RT-PCR data, an algorithm based on $\Delta C_T \geq 6$ representing ∼ 2-log or more increase in SARS-CoV-2 RNA following enrichment determines the presence of infectious virus in the sample (Fig. 1). Further, the method uses a short post-infection incubation (i.e., 9 h rather than multiple days), since complete host cell lysis is not required to determine RNA replication using differential RT-PCR analysis.

The method steps are shown in Fig. 2 with a description of these steps below.

2.5. RV-RT-PCR experiments with viral suspension

Experiments with viral suspension were conducted to determine the optimal infection period for RV-RT-PCR method development. The 96-well cell culture plates were prepared 18–24 h before an experiment as described above, with three or more wells per viral dilution and three wells for negative controls (without virus). The same plate layout was used for the T_0 plate and each timepoint plate (i.e., T_{12} and T_{24}). The plates were incubated at 37℃ with 5% CO_2 overnight, and the cell monolayer was allowed to become ∼100% confluent prior to addition of virus.

Viral suspensions were prepared by thawing an aliquot (stored at -80℃) from the titered-stock and adding 2% FBS DMEM to yield the desired viral concentrations (in 0.1 mL to be added per well) in 15-mL conical tubes. Sufficient volume was prepared for 10-fold viral dilutions to confirm the starting viral titer by conducting TCID50 analyses (with 12 replicates of 0.1 mL each for each 10-fold dilution). In some cases, 2-fold dilutions were also prepared for testing in RV-RT-PCR experiments to evaluate method sensitivity of detection.

Next, the medium was removed from cell-culture plates by multichannel pipettor (8- or 12-channel), taking care to not disturb the cells adhered to the bottom of the well, and 0.1-mL of the appropriate virus dilution (designated as sample) was added to wells. A 2% FBS DMEM aliquot (0.1-mL) was added to negative control wells. Plates were incubated at 37℃ with 5% CO_2 for 1- or 2-hr (with separate plates used for each combination of infection period/post-infection incubation period). At the end of each infection period, the medium was removed
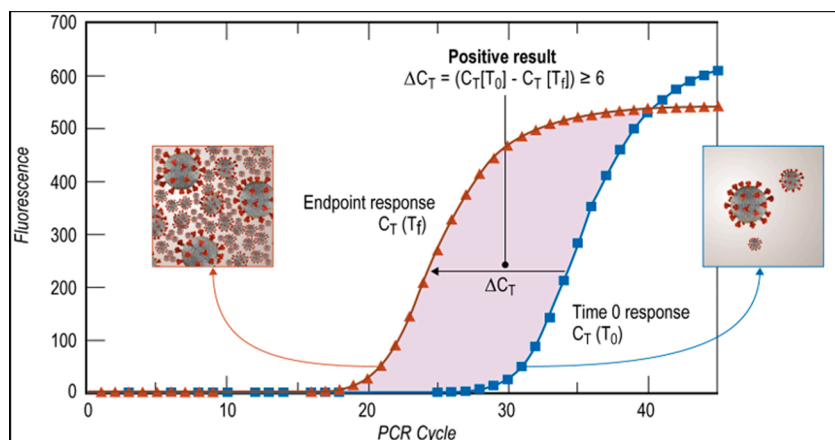

Fig. 1. Schematic of RT-PCR Response Curves from RV-RT-PCR Analysis of a Swab Sample.
The blue curve labeled "Time 0 response C_T (T_0)" represents the initial SARS-CoV-2 RT-PCR response for RNA from virions in the sample used to infect the cell culture (immediately after the infection period). The red curve labeled "Endpoint response C_T (T_f)" represents the SARS-CoV-2 RT-PCR response signifying viral propagation in cell culture and the resulting increase in RNA copies detected (shown by the increased quantity of virions in the red box relative to the blue box). Increased SARS-CoV-2 virions in cell culture result in increased SARS-CoV-2 RNA, which causes the RT-PCR response curve to shift to the left and produces a change in cycle threshold (C_T), or ΔC_T, where $\Delta C_T \geq 6$ indicates the presence of infectious virus in the sample.
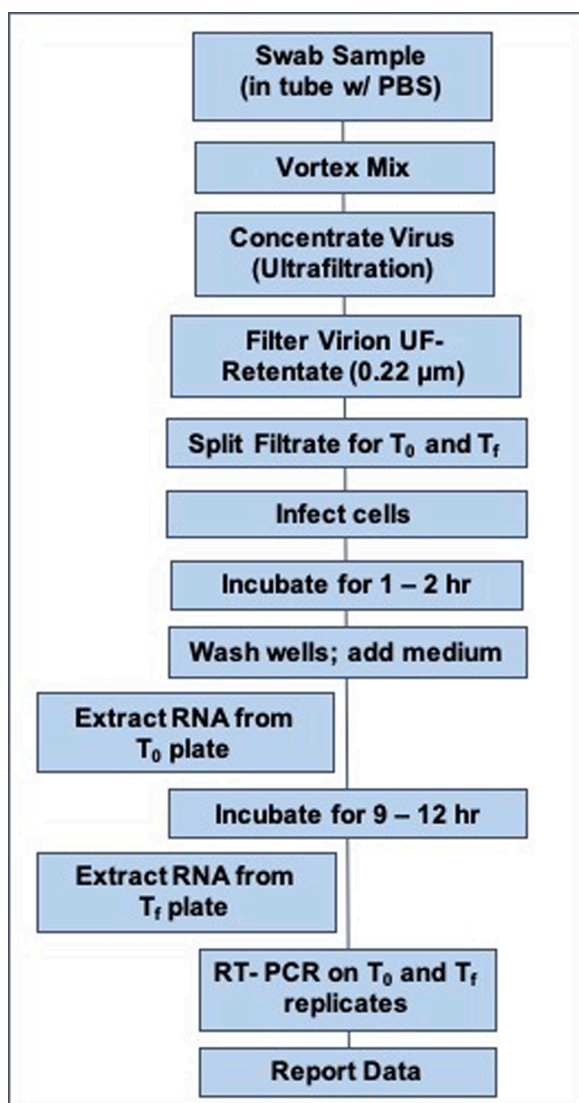
Fig. 2. RV-RT-PCR Method Development Flow Chart.
This schematic shows protocol steps used for mock swab swatch or swab samples spiked with different titers of SARS-CoV-2 for method development. Testing with viral suspension directly (not from swabs or swatches) started with the step labeled "Infect cells". The optimal infection and incubation periods were selected based on testing (as described in Sections 2.5 and 2.6, respectively). The 0.22-μm filtration step removes bacteria and fungi that could contaminate the cell-culture. UF = Ultrafiltration.

from the plate wells leaving the cell monolayer intact. Then, a wash step, addition of maintenance medium, and incubation was conducted (as described in Section 2.4) for 12-hr and 24-hr. For the T_0 plate and other plates at the end of the post-infection incubation period (e.g., 12-hr or 24-hr), the liquid volume was removed (leaving the monolayer intact) and 0.1-mL PBS were added to each well. The plate was then stored at -80°C until RNA extraction was conducted.

2.6. RV-RT-PCR experiments with swab swatches

Experiments with swab swatches spiked with different viral concentrations were conducted to determine the optimal post-infection incubation period for RV-RT-PCR method development. Since the Puritan swabs (Guilford, ME; Cat. No. P25-88060-PF-UW-DRY) previously used for environmental norovirus sampling were in high demand for SARS-CoV-2 response and resources were largely put into clinical swab

production, a sheet of the same foam material (~4–5 mm thick) was supplied by Puritan (as requested by CDC colleagues) to generate swatches for testing. Swatches were aseptically cut using sterile scissors into ~5 cm^2 (2.0 × 2.5 cm) pieces, approximately the same size as the Puritan swab head. The swatches (designated as samples) were then placed in individual 50-mL conical tubes. Triplicate tubes were prepared for each viral concentration as well as the negative control for analysis by RV-RT-PCR. Using the TCID50 analysis, viral recovery from spiked swatches was determined as follows: TCID50$_{sample}$ / TCID50$_{stock}$ (corrected for dilution) × 100 = percent recovery. The average % recovery with standard deviation was determined from triplicate swab swatches processed in parallel. Plaque forming units (PFU) were calculated from TCID50 data as described by Leibowitz et al. (2011): PFU = TCID50 × 0.7.

For RV-RT-PCR experiments, swatches were prepared by pre-wetting with 1.5-mL PBS. To the pre-wetted swatches, 0.5 mL of the appropriate viral stock dilution was spiked. Then, 8-mL PBS was added for virion recovery, making the total volume 10-mL (since swabs used for surface sampling are typically shipped in 10-mL buffer). The tubes were then vortexed at ~3200 rpm in 15 s bursts with 1–2 seconds in between for 1 min. Next, each swatch recovered suspension was concentrated by ultrafiltration using Amicon® Ultra-15 Centrifugal Filter Units with 10 kDa MWCO membranes (Sigma-Aldrich, Allentown, PA; Cat. No. UFC901096). The swatch recovered suspensions (~8–8.5 mL each) in Ultra-15 UF tubes were centrifuged at 4000 rpm (~3200 × g) using an Eppendorf 5810R centrifuge (Eppendorf, Enfield, CT) with 50-mL tube rotor adapters, for ~17 min at 4°C to bring the volume down to 0.3–0.5 mL. For all tubes, the volume was brought to 0.5-mL using sterile PBS. The 0.5-mL retentate was then filtered through a sterile 0.22-μm filter (Millipore®, Burlington, MA; Cat. No. UFC30GV0S) by centrifuging at 7000 rpm for 1 min to remove any bacterial or fungal contaminants. The RV-RT-PCR infection and incubation steps for swatch samples were as described above for viral suspension (Section 2.5); however, since swatch filtrates were in PBS, 0.1-mL 2% FBS DMEM was also added to each well to provide proper medium conditions for viral infection.

A larger retentate volume of 0.5-mL was used for method development to enable testing of multiple post-infection incubation periods (T_0, T_9, T_{12}, etc.) from the same swatch UF-retentate, with 0.1-mL used for each incubation timepoint. For these experiments, an 0.1-mL aliquot was also available for TCID50 analysis from the same swatch UF-retentate, with 10-fold dilutions prepared in 2% FBS DMEM as described above.

2.7. RV-RT-PCR experiments with swabs for SARS-CoV-2

The protocol for swatches was used for experiments with Sani-MacroSwabs (Sanigen, Anyang, Gyeonggi-do, South Korea; www.sanigen.kr), which were made from similar materials to the Puritan swabs. In this case, swab tubes already contained 10-mL PBS with the swab shaft attached to the tube cap; therefore, 0.5 mL was removed prior to adding the viral dilution to the swab head and placing it back into the tube with PBS (mimicking how a surface sample would be processed). For this evaluation of the final RV-RT-PCR method, the UF-retentate volume was decreased from 0.5-mL to ~0.2-mL, which was split evenly between T_0 and T_f (T_9) analyses. As for viral suspension experiments, the starting viral concentrations for the two replicate swab experiments varied slightly based on different starting viral titers and viral recovery efficiencies (determined from swab samples processed in parallel for TCID50 analysis). These replicate swabs for TCID50 analysis were processed in the same way as those used for RV-RT-PCR analysis, and results were related to the titer of the viral stock to determine the percent recovery as described in Section 2.6. Furthermore, % recoveries from higher viral concentrations were averaged and used to estimate a starting viral concentration per swatch for lower viral concentrations where % recovery was not determined directly, since these concentrations were often typically below the TCID50 method detection limit.

2.8. RNA extraction

The MagneSil® Total RNA Mini Isolation System (Promega; Madison, WI; Cat. No. Z3351) was used for extraction of viral RNA from cell culture following the manufacturer's protocol; however, the protocol was adapted for manual extraction using 2-mL tubes with a DynaMag™-2 Magnetic Rack (Thermo Fisher Scientific, Grand Island, NY; Cat. No. 12321D). The starting materials for extraction were individual wells on 96-well plates that contained a cell monolayer infected with virus and covered with 0.1 mL PBS. The plates were stored at -80°C at the appropriate timepoint (i.e., T_0 or T_f) for RV-RT-PCR analysis. While still frozen, 0.1 mL RNA Lysis Buffer was added to each well to be extracted. Once thawed, the well contents with Lysis Buffer were pipetted up and down to mix prior to transferring to a RNase-free 2-mL snap-cap tube. The Magnesil protocol included a step with DNase I treatment, followed by additional wash steps, and final elution in 50 μL nuclease-free water with 0.5 μL RNasin® Plus RNase Inhibitor (Promega; Cat. No. N2611, 2500 units) or 0.125 μL RNasin Plus RNase Inhibitor (Promega; Cat. No. N2615, 10,000 units). If not analyzed immediately by RT-PCR, RNA extracts were stored at -80°C for up to 5 days.

2.9. SARS-CoV-2 RT-PCR analysis

For real-time RT-PCR analysis of SARS-CoV-2, the N1 assay was used for method development and both N1 and N2 assays (Lu et al., 2020) were used for the final RV-RT-PCR method evaluation with spiked swabs. The primers and probes were supplied by Biosearch Technologies (Novato, CA; Cat. No. KIT-NCOV-PP1−1000). Ten-fold dilutions of a synthetic RNA standard (BEI Resources; Cat. No. NR-52358), resulting in levels ranging from 1.5 to 1.5×10^5 viral genome copies per RT-PCR reaction, were run with each PCR plate along with a negative control (nuclease-free water only).

Each 25-μL RT-PCR reaction contained 12.5-μL 2X Master Mix and 0.5-μL ROX Dye II (One Step PrimeScript™ III RT-PCR Kit; Takara Bio, Mountain View, CA; Cat. No. RR600B), 0.625-μL primers/probe (5 μM probe, 20 μM each forward and reverse primers), 6.375-μL PCR-grade water, and 5-μL RNA extract. An Applied Biosystems 7500 Fast Real-Time PCR Instrument (Thermo Fisher Scientific) was used with the following thermocycling conditions: 50°C for 15 min; 95°C for 2 min; 45 cycles of 95°C for 3 s and 55°C for 30 s.

2.10. RV-RT-PCR data analysis and results interpretation

RV-RT-PCR algorithm for a positive virus detection result: An average C_T was determined from triplicate PCR reactions for T_0 and T_f RNA extracts of each sample. The average C_T of the T_f RNA extract was subtracted from the average C_T of the T_0 RNA extract to determine the average ΔC_T for the sample. The pooled SD for the average ΔC_T was calculated as the square root of the following: (SD for $C_T(T_0)$ values squared plus the SD for the $C_T(T_f)$ values squared)/2, where T_f is the final number of hours post-infection. An algorithm based on an approximately 2-log or more increase in viral RNA following enrichment was applied such that the resultant $\Delta C_T \geq 6$ determined the presence of infectious virus in the sample.

If there was no C_T for the T_0 or T_f RNA extracts (i.e., the result was non-detect), the C_T was set to 45 (the total number of PCR cycles used) in order to calculate a ΔC_T value. A minimum of two out of three T_0 PCR replicates with C_T values $\leq$ 44 (in a 45-cycle PCR) was required to calculate the average C_T. In addition, for the sample RT-PCR data to be valid, (i) the negative controls could not yield any measurable C_T values (i.e., a minimum of 2 of 3 RT-PCR replicates needed to be non-detect), and (ii) no-template RT-PCR controls could not yield measurable C_T values.

RV-RT-PCR analysis of sample replicates (for method development): Triplicate samples (virus suspension dilution, swab swatches or swabs) were used for each test condition (i.e., viral concentration, infection period, and post-infection incubation period combination). An

overall average C_T value was calculated from the individual sample average C_T values. If only two sample replicates had C_T values (to calculate an average C_T) and the third sample replicate was "non-detect", the overall average C_T was calculated from the two samples with average C_T values. The overall standard deviation (SD) was calculated from the following equation for 3 of 3 positive sample replicates (with average C_T values):

$$\text{Overall or joint SD} = \sqrt{\{[(n_1-1)s_1{}^2 + (n_2-1)s_2{}^2 + (n_3-1)s_3{}^2 + (n_1 \times [X_1 - \overline{X}]^2) + (n_2 \times [X_2 - \overline{X}]^2) + (n_3 \times [X_3 - \overline{X}]^2)]/(n_1 + n_2 + n_3 - 1)\}}$$

where n_1, n_2, and n_3 = the number of RT-PCR analyses per sample for sample replicates 1, 2, and 3; s_1, s_2, and s_3 = the standard deviation (SD) of the C_T values for the individual samples; X_1, X_2, and X_3 = the average C_T values for the individual samples; $\overline{X}$ = the overall average C_T value for the samples. The overall SD equation was modified accordingly for only two sample replicates with C_T values. The overall SD equation was also used to determine the overall SD for average ΔC_T from triplicate swatch or swab samples spiked with the same viral concentration.

2.11. Biosafety

All work with SARS-CoV-2 cultures were done under Biosafety Level 3 (BSL-3) conditions following Federal Select Agent Program regulations, including use of a certified Class II biosafety cabinet, with thimble connection and ducted exhaust, and the following personal protective equipment (PPE): Powered Air Purifying Respirator (PAPR), Tyvek coverall with hood and boots, disposable apron, Tyvek sleeves, shoe covers, and double latex or nitrile gloves. Aerosolization risk was mitigated by use of aerosol barrier tips during pipetting and use of removable, gasketed safety cups for centrifugation that could be loaded/unloaded in the biosafety cabinet. Secondary containment was used for 96-well plates during incubation. Waste was subjected to two rounds of sterilization using a certified and permitted autoclave, documented at 15 psi and 121°C for $\geq$ 60 min prior to disposal.

3. Results

3.1. RV-RT-PCR analysis of SARS-CoV-2 suspension

The RV-RT-PCR results for viral suspension studies with 2-hr infection and 12- or 24-hr post-infection incubation (or simply, incubation) are summarized in Table 1 for two replicate experiments with different starting viral concentrations. The T_0 and T_f C_T values for triplicate RT-PCR analyses from these experiments are included in Supplemental Tables S1–S3. The average ΔC_T data for T_{12} incubation showed 3 of 3 positive replicates ($\Delta C_T \geq 6$) down to 44 PFU/sample. Below this viral concentration, 2 of 3 were positive for ~25 PFU/sample with average ΔC_T of 12.3 for one experiment; whereas, 3 of 3 were positive for ~4 PFU/sample with average ΔC_T of 23.0 for the other experiment.

RV-RT-PCR analysis with 1-hr infection (and 12-hr or 24-hr incubation) was also assessed in one of the experiments, showing similar trends to that for 2-hr infection/12-hr incubation with 3 of 3 positive for ~248 PFU/sample (avg. $\Delta C_T = 11.5 \pm 0.3$) and 2 of 3 positive for ~25 PFU/sample (avg. $\Delta C_T = 12.7 \pm 2.1$); however, with 24-hr incubation, 2 of 3 were positive for ~25 PFU/sample for 1-hr infection (avg. $\Delta C_T = 21.3 \pm 2.0$; Supplemental Table S3). Therefore, a 2-hr infection period was selected for subsequent experiments focused on determining an optimal incubation period to achieve a better method sensitivity for actual environmental samples, which may contain low viral concentrations and interferents that negatively impact viral infection.

3.2. RV-RT-PCR analysis of SARS-CoV-2-spiked swab swatches

Once the infection period was established (i.e., 2-hr), experiments were conducted using swab swatches to determine an optimal incubation period for method sensitivity. The same swab swatch with

Table 1
Summary of RV-RT-PCR Avg. ΔC_T Results from Replicate Experiments for SARS-CoV-2-Infected Vero E6 Cells with 2-hr Infection.

Estimated PFU/ Sample (T_0 and T_f aliquots)[a]	T_{12} Avg. ΔC_T (SD)[b]	T_{12} Positive Results	T_{24} Avg. ΔC_T (SD)[b]	T_{24} Positive Results
440	12.5 ± 0.1	3 of 3	15.2 ± 0.2	3 of 3
248	13.7 ± 0.6	3 of 3	18.7 ± 0.6	3 of 3
44	13.0 ± 4.1	3 of 3	15.7 ± 4.4	3 of 3
25	12.3 ± 0.8	2 of 3	17.4 ± 0.8	3 of 3
4	23.0 ± 1.6	3 of 3	23.0 ± 5.7	3 of 3

PFU = Plaque Forming Units; TCID50 = 50% Tissue Culture Infectious Dose; C_T = Cycle Threshold; Avg. = Average; SD = Standard Deviation.

[a] Values are based on dilution of the SARS-CoV-2 titered stock suspension and volume of dilution used for T_0 and T_f plate wells (0.1 mL each). Viral titer data is included in Supplemental Tables S1–S3. Estimated PFU/Sample = TCID50/Sample (corrected for dilution) × 0.7.

[b] Avg. and SD are based on three replicates unless specified in the "Positive Results" column. SD represents the pooled SD which equals the square root of the following: (SD for T_0 values squared plus the SD for the T_f values squared)/2.

recovered suspension was used for both RV-RT-PCR and TCID50 analyses. Swatches were spiked using 0.5 mL from -3 and -3.3 $\log_{10}$ viral dilutions of the titered SARS-CoV-2 stock in triplicate. Based on the TCID50 analysis of the viral stock used for this experiment (TCID50 $10^{5.17}$/0.1 mL or ~1.03×10^5 PFU/0.1 mL), ~514 and ~257 PFU were added per swatch for the respective viral dilutions. Triplicate negative controls without virus were processed in parallel.

After swatch processing, 0.5 mL UF-retentate was obtained, and 0.1 mL aliquots were added to T_0, T_9, and T_{12} cell culture plates. Additionally, 0.1 mL was used for TCID50 analysis (Section 2.3). Because actual sample analysis will use the entire recovered viral UF-retentate (0.2 mL), split into only two parts (0.1 mL each) for T_0 and T_f, the "PFU for RV-RT-PCR Analysis" for this experiment are expressed based on 0.2 mL (Table 2), rather than 0.1 mL used for TCID50 analysis of swatch UF-retentates (Supplemental Table S4). Therefore, the "PFU for RV-RT-PCR Analysis" ranged from ~44 to 140 and ~14 to 79 for the 514 and 257 PFU/swatch concentrations, respectively. The RV-RT-PCR results with 9-hr (T_9) incubation showed 3 of 3 positive samples for each PFU/swatch concentration with average ΔC_T values of 10.5 ± 0.6 and 9.4 ± 1.6 for ~514 and ~257 PFU/swatch, respectively (Table 2, top half); therefore, 12-hr (T_{12}) aliquots were not analyzed. Results for the negative control were non-detect (data not shown). The T_0 and T_9 C_T values for triplicate RT-PCR analyses from these experiments are included in Supplemental Table S5 (for the first experiment) and Table S7 (for the replicate experiment described below).

The replicate experiment used a titered SARS-CoV-2 stock with TCID50 of $10^{4.6}$/0.1 mL or ~2.68×10^4 PFU/0.1 mL. Likewise, for ~134 PFU/swatch (~25 PFU for RV-PTPCR analysis), 3 of 3 replicates were detected with average ΔC_T of 8.1; whereas, for the lower viral concentration of ~67 PFU/swatch (Avg. ~11 PFU for RV-PT-PCR analysis), 2 of 3 replicates were detected with an average ΔC_T of 9.8 (Table 2, bottom half). Results from TCID50 analysis are included in Supplemental Table S6 and results for the negative control swatches were non-detect (data not shown). Based on TCID50 analysis of swatch UF-retentates, the PFU available for RV-RT-PCR analysis (split between T_0 and T_9 sample wells) was ~25 and ~8 – 14 for the 134 and 67 PFU/swatch concentrations, respectively (for 2 of 3 swatch replicates). Since 2 of 3 T_9 swatch sample replicates showed positive ΔC_T values (8.3–11.4) for the ~67 PFU/swatch concentration, T_{12} sample wells were not analyzed.

Testing with swab swatches showed that after a 2-hr infection period, a 9-hr incubation period allowed sufficient viral propagation. These results suggest if the entire swatch UF-retentate was processed for RV-RT-PCR analysis, estimated starting PFU/swatch concentrations of ~67 or lower could be reliably detected by RV-RT-PCR analysis. Furthermore, an estimated ~14 "PFU for RV-RT-PCR Analysis" resulted

Table 2
RV-RT-PCR and TCID50 Results from Replicate Experiments for SARS-CoV-2-Spiked Swab Swatches Processed and Used to Infect Vero E6 Cells with 2-hr Infection.

Estimated PFU/Swatch[a]	Swatch Replicate	PFU for RV-RT-PCR Analysis[b]	Avg. C_T (SD)[c] After 2-hr Infection T_0	Avg. C_T (SD)[c] After 2-hr Infection T_9	Avg. ΔC_T (SD)[d]
	1	44	32.5 (0.2)	21.3 (0.1)	11.2 (0.2)
	2	140	32.2 (0.1)	22.4 (0.04)	9.8 (0.1)
514	**3**	79	31.8 (0.1)	21.3 (0.1)	10.5 (0.1)
	Overall Avg. (SD)	**88 (49)**	**32.2 (0.3)**	**21.7 (0.6)**	**10.5 (0.6)**
	1	79	33.1 (0.2)	25.5 (0.04)	7.6 (0.1)
	2	14	33.6 (0.2)	22.5 (0.03)	11.2 (0.1)
257	**3**	25	33.3 (0.2)	23.9 (0.1)	9.4 (0.2)
	Overall Avg. (SD)	**39 (35)**	**33.3 (0.3)**	**24.0 (1.3)**	**9.4 (1.6)**
Replicate Experiment					
	1	25	32.9 (0.1)	23.1 (0.04)	9.7 (0.09)
	2	(>56)	34.0 (0.4)	26.3 (0.1)	7.6 (0.3)
134	**3**	25	33.5 (0.4)	26.6 (0.02)	6.8 (0.3)
	Overall Avg. (SD)	**24.9 (0)**	**33.4 (0.5)**	**25.4 (1.7)**	**8.1 (1.8)**
	1	14	35.1 (0.1)	26.8 (0.1)	8.3 (0.1)
	2	(>28)	35.1 (0.5)	23.7 (0.02)	11.4 (0.3)
67	**3**	8	35.5 (0.1)	36.0 (0.2)	−0.5 (0.2)
	Overall Avg. (SD) (3 Reps)	**NA**	**35.2 (0.3)**	**28.8 (5.5)**	**6.4 (5.3)**
	Overall Avg. (SD) (2 Reps)	**10.9 (4.3)**	**35.1 (0.3)**	**25.3 (1.7)**	**9.8 (1.7)**

PFU = Plaque Forming Units; TCID50 = 50% Tissue Culture Infectious Dose; C_T = Cycle Threshold; Avg. = Average; SD = Standard Deviation; NA = Not Applicable; Reps = Replicates.

[a] Values are based on dilutions from a TCID50-titered SARS-CoV-2 stock. For 514 and 257 PFU/Swatch: average TCID50 = $10^{5.17}$/0.1 mL or ~1.03×10^5 PFU/0.1 mL. TCID50/0.1 mL with SD = 0.99–2.17 × 10^5 and PFU/0.1 mL with SD = 0.69–1.52 × 10^5. For 134 and 67 PFU/Swatch: average TCID50 $10^{4.6}$/0.1 mL or ~2.68×10^4 PFU/0.1 mL. TCID50/0.1 mL with SD = 3.2–4.6 × 10^4 and PFU/0.1 mL with SD = 2.2–3.25 × 10^4. Estimated PFU/Swatch = TCID50/Swatch (corrected for dilution) × 0.7.

[b] Values are based on TCID50 analysis of swatch UF-retentates using 0.2 mL as the total volume since 0.1 mL was used for T_0 and 0.1 mL was used T_9 for RV-RT-PCR analysis. Values with greater than 100% recovery are shown as greater than 100% PFU for 0.2 mL.

[c] Avg. C_T and SD are based on triplicate RT-PCR analyses from triplicate swatch samples per viral concentration.

[d] SD represents the pooled SD which equals the square root of the following: (SD for T_0 values squared plus the SD for the T_9 values squared)/2.

in positive results with average ΔC_T values of 8.3 and 11.2 (Table 2), well above the $\Delta C_T \geq 6$ requirement for positive detection.

3.3. Analysis of SARS-CoV-2-spiked swab samples using the optimized RV-RT-PCR method

Using the optimized RV-RT-PCR method as described above (specifically with 2-hr infection/9-hr incubation), actual swabs (Sani-MacroSwab) were tested with three SARS-CoV-2 dilutions including -3, -3.3, and -4 $\log_{10}$ relative to the virus stock (TCID50 $10^{5.25}$/0.1 mL or ~1.24

$\times 10^5$ PFU/0.1 mL), along with a negative control (without virus), using triplicate swabs per viral concentration or negative control. Swabs were processed as described for swab swatches; however, after vortex-mixing the tube, the recovered swab suspension (with virus) was concentrated by UF to ~0.2 mL instead of 0.5 mL and split in half between the appropriate cell-culture wells on T_0 and T_9 plates, as for actual swab sample analysis, and processed as described (Section 2.7). In addition, recovery efficiency was determined separately by conducting TCID50 analysis of replicate swabs spiked with -2 and -3 $\log_{10}$ viral dilutions in triplicate. Recovery efficiency data was used to determine estimated PFU/swab concentrations.

RV-RT-PCR results using the N1 and N2 assay for the first experiment are shown in Table 3; the negative control replicates were non-detect for both assays (data not shown). The estimated PFU/swab based on TCID50 analysis of the viral stock (~1.24×10^5 PFU/0.1 mL) were approximately 620, 310, and 62 for the three viral dilutions (Supplemental Table S8). The N1 assay data showed positive RV-RT-PCR results for 3 of 3 swab replicates after 2-hr infection and 9-hr incubation for all three starting viral concentrations. Average ΔC_T values for N1 were 11.0 ± 0.6, 10.9 ± 0.2, and 12.7 ± 0.6 for ~620, ~310, and ~62 estimated PFU/swab, respectively. RV-RT-PCR results using the N2 assay also showed 3 of 3 swab replicates positive for all three virus concentrations with average ΔC_T values of 11.5 ± 0.6, 11.2 ± 0.2, and 13.1 ± 0.5 for ~620, ~310, and ~62 estimated PFU/swab, respectively. The T_0 and T_9 C_T values for triplicate RT-PCR analyses from these experiments are included in Supplemental Table S9 (N1 Assay) and Table S10 (N2 Assay). The data showed a less than 50 virions sensitivity of detection could be achieved with RV-RT-PCR analyses using the N1 and N2 assays.

A replicate experiment was conducted with swabs using the optimized RV-RT-PCR method as described above; however, in this case, -3.3, -4, and -4.3 $\log_{10}$ dilutions relative to the virus stock (TCID50 $10^{5.0}$/0.1 mL or ~7×10^4 PFU/0.1 mL) were used. As for the first experiment, viral recovery efficiency was also determined by TCID50 analysis of swabs spiked with -2 and -3 $\log_{10}$ viral dilutions in triplicate, to estimate PFU/swab concentrations (Supplemental Table S11).

RV-RT-PCR results using the N1 and N2 assay for the replicate experiment are shown in Table 4; the negative control replicates were non-detect for both assays (data not shown). The T_0 and T_9 C_T values for triplicate RT-PCR analyses from these experiments are included in Supplemental Table S12 (N1 Assay) and Table S13 (N2 Assay). The estimated PFU/swab based on TCID50 analysis of the viral stock were approximately 175, 35, and 18 (Supplemental Table S11) for the three different viral dilutions based on the titer of the SARS-CoV-2 stock (avg. 7.0×10^4 PFU/0.1 mL). The data showed positive RV-RT-PCR results for 3 of 3 swab replicates after 2-hr infection and 9-hr incubation for two of the three starting viral concentrations, with ΔC_T values > 6 for ~175 and ~35 PFU/swab concentrations, although the lowest virus concentration (~18 PFU/swab) was negative for all three swab replicates. The results were similar for the N2 assay. Average ΔC_T values were 11.4 and 11.8 for the N1 and N2 assays, respectively for ~175 PFU/swab and

13.3 and 14.1 for the N1 and N2 assays, respectively for ~35 PFU/swab.

4. Discussion

The SARS-CoV-2 RV-RT-PCR method was optimized with regard to: (i) 96-well Vero E6 cell culture density; (ii) swab processing by vortex-mixing, ultrafiltration concentration (up to ~50-fold volume reduction so entire sample can be used for RV-RT-PCR analysis), and 0.22-micron filtration to remove microbial contaminants; (iii) sample splitting between T_0 and T_9 wells/plates; (iv) viral infection period (2-hr with potential for a shorter time period); (v) post-infection viral incubation period (9-hr with flexibility for longer time periods for complex samples); (vi) RNA extraction using a readily-available commercial kit compatible with automation; and (vii) use of established RT-PCR assays with flexibility for other assays of interest.

The results of this study demonstrated this method can provide accurate, sensitive data for the presence of infectious SARS-CoV-2 in swab samples in hours rather than days required for current laborious TCID50 or plaque assays (Riddell et al., 2020; Pastorino et al., 2020; Ben-Shmuel et al., 2020). With front-end sample processing (~3-hr), 2-hr infection, 9-hr incubation, RNA extraction and RT-PCR analysis (~3-hr), the total time to results was ~17 h (for a batch of 12 swabs). For environmental samples containing non-target viruses, a specific and sensitive SARS-CoV-2 RV-RT-PCR method would provide more definitive results compared to subjective culture-based methods relying on CPE or plaque formation, for which RT-PCR confirmation may be required. In this study, results showed that even for low starting viral concentrations, the method algorithm of $\Delta C_T \geq 6$ for a positive result was satisfactorily met for replicate swab samples.

Similar to the RV-RT-PCR approach, the integrated cell culture-PCR (ICC-PCR) methods for other viruses also combined virus enrichment in cell-culture with PCR (Reynolds et al., 2001; Gallagher and Margolin, 2007; Rigotto et al., 2010), although only endpoint PCR or RT-PCR was performed. Conversely, the RV-RT-PCR method uses RT-PCR analysis for SARS-CoV-2 RNA before and after the post-infection cell-culture-virus (sample) incubation to determine the C_T difference (ΔC_T) to distinguish infectious from noninfectious virus. Further, with 9-hr incubation, the RV-RT-PCR method is more rapid compared to a reported method (Zhou et al., 2020) that also performed RT-PCR analysis before and after post-infection incubation, but used 5–7 days post-infection to obtain results. A shorter incubation period not only enhances sample throughput, it also means RNA is extracted while viral genomes are still undergoing replication, rather than extracting only the post-cell-lysis supernatant after multiple days of infection, where viral RNA levels may be declining. In addition, the criteria for positive determination by RV-RT-PCR is more stringent, as the algorithm for presence of infectious virus requires a ~two-log increase in the viral RNA during a 9-hr post-infection incubation (at least 6 C_T decrease) compared to one-log after 5–7 days post-infection reported by Zhou et al. (2020).

Based on the results of this study, an estimated timeline for RV-RT-

Table 3
RV-RT-PCR Results for SARS-CoV-2-Spiked Swabs Processed and Used to Infect Vero E6 Cells with 2-hr Infection and 9-hr Post-Infection Incubation – N1 and N2 Assays.

Estimated PFU/ Swab[a]	Avg. C_T (SD)[b] for N1 Assay by Post-Infection Incubation Timepoint		N1 Assay Avg. ΔC_T (SD)[c]	N1 Positive Results	Avg. C_T (SD)[b] for N2 Assay by Post-Infection Incubation Timepoint		N2 Assay Avg. ΔC_T (SD)[c]	N2 Positive Results
	T_0	T_9			T_0	T_9		
620	31.0 (0.3)	20.0 (0.8)	11.0 (0.6)	3 of 3	30.3 (0.4)	18.8 (0.7)	11.5 (0.6)	3 of 3
310	32.0 (0.2)	21.1 (0.2)	10.9 (0.2)	3 of 3	31.3 (0.2)	20.1 (0.4)	11.2 (0.2)	3 of 3
62	35.3 (0.5)	22.7 (0.5)	12.7 (0.6)	3 of 3	34.7 (0.7)	21.6 (0.6)	13.1 (0.5)	3 of 3

PFU = Plaque Forming Units; TCID50 = 50% Tissue Culture Infectious Dose; C_T = Cycle Threshold; Avg. = Average; SD = Standard Deviation.
[a] Values are based on dilutions from a TCID50-titered SARS-CoV-2 stock (TCID50 $10^{5.25}$/0.1 mL or ~1.24×10^5 PFU/0.1 mL). Estimated PFU/Swab = TCID50/Swab (corrected for dilution) $\times$ 0.7.
[b] Avg. C_T and SD are based on triplicate RT-PCR analyses from triplicate swab samples per viral concentration.
[c] SD represents the pooled SD which equals the square root of the following: (SD for T_0 values squared plus the SD for the T_9 values squared)/2.

Table 4

RV-RT-PCR Results for SARS-CoV-2-Spiked Swabs Processed and Used to Infect Vero E6 Cells with 2-hr Infection and 9-hr Post-Infection Incubation – N1 and N2 Assays (Replicate Experiment).

Estimated PFU/Swab[a]	Avg. C_T (SD)[b] for N1 Assay by Post-Infection Incubation Timepoint		N1 Assay Avg. ΔC_T (SD)[c]	N1 Positive Results	Avg. C_T (SD)[b] for N2 Assay by Post-Infection Incubation Timepoint		N2 Assay Avg. ΔC_T (SD)[c]	N2 Positive Results
	T_0	T_9			T_0	T_9		
175	30.0 (0.2)	18.7 (0.6)	11.4 (0.8)	3 of 3	28.4 (0.1)	16.6 (0.7)	11.8 (0.8)	3 of 3
35	33.3 (0.5)	19.9 (0.4)	13.3 (0.4)	3 of 3	31.7 (0.5)	17.6 (0.4)	14.1 (0.4)	3 of 3
18	33.2 (0.5)	36.3 (1.7)	−3.1 (1.4)	0 of 3	31.5 (0.4)	34.5 (1.1)	−3.0 (0.7)	0 of 3

PFU = Plaque Forming Units; TCID50 = 50% Tissue Culture Infectious Dose; C_T = Cycle Threshold; Avg. = Average; SD = Standard Deviation.

[a] Values are based on dilutions from a TCID50-titered SARS-CoV-2 stock. (TCID50 $10^{5.0}$/0.1 mL or ~7×10^4 PFU/0.1 mL). Estimated PFU/Swab = TCID50/Swab (corrected for dilution) × 0.7.

[b] Avg. C_T and SD are based on triplicate RT-PCR analyses from triplicate swab samples per viral concentration.

[c] SD represents the pooled SD which equals the square root of the following: (SD for T_0 values squared plus the SD for the T_9 values squared)/2.

PCR-based analysis of swab samples is shown in Fig. 3. The timeline is shown for 22 samples plus controls, although the method's 96-well plate format has the potential for higher throughput capacity, where up to 96 samples and controls can be processed in two 96-well cell culture plates, one for T_0 and one for T_9. Such increased sample quantity, however, would increase the time-to-results for triplicate RT-PCR analyses for T_0 and T_9 for each sample, unless multiple PCR instruments were available. Furthermore, this timeline does not include initial Vero E6 cell growth and plating at optimum cell density. However, it is assumed that during an ongoing infection spread, the analytical laboratory would keep 96-well cell-culture plates ready for anticipated sample analysis.

The multi-well plate format used in this method also enables a small footprint, which is highly desirable in a BSL-3 laboratory. This format requires less incubator space and generates less hazardous waste from (i) significantly fewer multi-well plates compared to cell-culture flasks/plates required for traditional methods, (ii) lower volumes of growth medium and reagents, and (iii) predominant use of micropipette tips for small volumes rather than large serological pipets used for traditional methods.

The RV-RT-PCR method developed using the non-human primate kidney cell line, Vero E6, can also be adapted to various human cell lines for potential application for efficacy testing of antibody-based vaccines and anti-viral drugs, since more rapid and potentially more sensitive results can be obtained compared to current culture-based methods. Further, since the propagation of virus through traditional cell culture creates a potential selection pressure, especially as cultures are prolonged, this rapid method may be useful for characterization of SARS-CoV-2 variants via specific RT-PCR assays. Finally, the method can also serve as a model for developing rapid methods for other viruses of concern including both bioterrorism and public health threats.

5. Conclusions

In the wake of the rapid, world-wide spread of the COVID-19 pandemic, a RV-RT-PCR method was developed in a 96-well format to detect infectious SARS-CoV-2 in swab samples in less than a day to help understand surface stability and potential transmission for epidemiological investigations. The RV-RT-PCR method integrates cell-culture-based enrichment of SARS-CoV-2 in a sample with viral gene-specific RT-PCR-based molecular analysis conducted before and after a short (9-hr) incubation to determine the presence of infectious virus based on $\Delta C_T \geq 6$ (representing ~ 2-log or more increase in the SARS-CoV-2 RNA). Since post-infection-RT-PCR analysis is performed while the virus is replicating in the host cells and not after complete cell lysis, the method time-to-results is less than one day with detection sensitivity of <50 virions per swab sample.

Author statement

Sanjiv R. Shah: Conceptualization; Project administration; Methodology; Formal Analysis; Writing – Original and Review & Editing; Funding acquisition.

Staci R. Kane: Conceptualization; Project administration; Methodology; Formal Analysis; Writing support – Original and Review & Editing.

Maher Elsheikh: Investigation; Formal Analysis.

Teneile Alfaro: Investigation.

All authors are in agreement for publication of this manuscript.
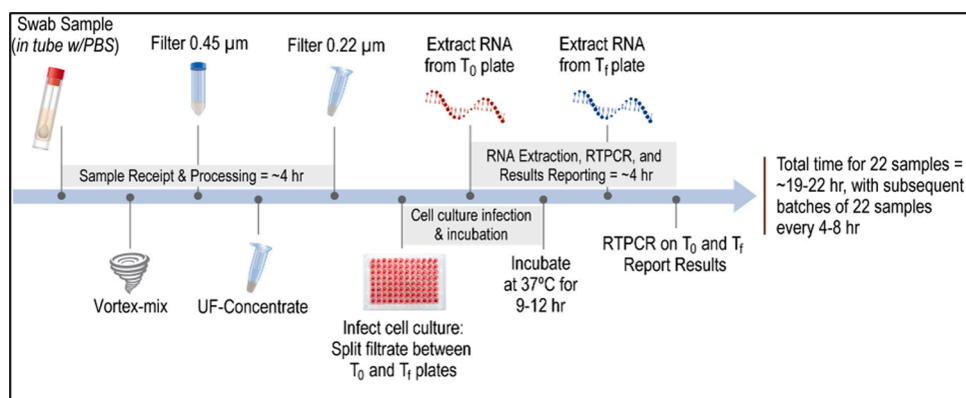
Declaration of Competing Interest

None.

Fig. 3. Estimated Timeline for RV-RT-PCR-Based Swab Sample Analysis.

Appendix A. Supplementary data

Supplementary material related to this article can be found, in the online version, at https://doi.org/10.1016/j.jviromet.2021.114251.

References

Aboubakr, H.A., Sharafeldin, T.A., Goyal, S.M., 2020. Stability of SARS-CoV-2 and other coronaviruses in the environment and on common touch surfaces and the influence of climatic conditions: a review. Transbound. Emerg. Dis. 68 (2), 296–312. https://doi.org/10.1111/tbed.13707.

Agol, V.I., Belov, G.A., Bienz, K., Egger, D., Kolesnikova, M.S., Raikhlin, N.T., Romanova, L.I., Smirnoa, E.A., Tolskaya, E.A., 1998. Two types of death of poliovirus-infected cells: caspase involvement in the apoptosis but not cytopathic effect. Virology 252 (2), 343–353. https://doi.org/10.1006/viro.1998.9438.

Arons, M.M., Hatfield, K.M., Reddy, S.C., Kimball, A., James, A., Jacobs, J.R., Taylor, J., Spicer, K., Bardossy, A.C., Oakley, L.P., Tanwar, S., Dyal, J.W., Harney, J., Chisty, Z., Bell, J.M., Methner, M., Paul, P., Carlson, C.M., McLaughlin, H.P., Thornburg, N., Tong, S., Tamin, A., Tao, Y., Uehara, A., Harcourt, J., Clark, S., Brostrom-Smith, C., Page, L.C., Kay, M., Lewis, J., Montgomery, P., Stone, N.D., Clark, T.A., Honein, M.A., Duchin, J.S., Jernigan, J.A., 2020. Presymptomatic SARS-CoV-2 infections and transmission in a skilled nursing facility. N. Engl. J. Med. 382, 2081–2090. https://doi.org/10.1056/NEJMoa2008457.

Avanzato, V.A., Matson, M.J., Seifert, S.N., Pryce, R., Williamson, B.N., Anzick, S.L., Barbian, K., Judson, S.D., Fischer, E.R., Martens, C., Bowden, T.A., de Wit, A., Riedo, F.X., Munster, V.J., 2020. Case Study: prolonged infectious SARS-CoV2 shedding from an asymptomatic immunocompromised individual with cancer. Cell 183, 1901–1912. https://doi.org/10.1016/j.cell.2020.10.049.

Bedrosian, N., Mitchell, E., Rohm, E., Rothe, M., Kelly, C., String, G., Lantagne, D., 2020. A systematic review of surface contamination, stability, and disinfection data on SARS-CoV-2 (Through July 10, 2020). Environ. Sci. Technol. 55 (7), 4162–4173. https://doi.org/10.1021/acs.est.0c05651.

Ben-Shmuel, A., Brosh-Nissimov, T., Glinert, I., Bar-David, E., Sittner, A., Poni, R., Cohen, R., Achdout, H., Tamir, H., Yahalom-Ronen, Y., Politi, B., Melamed, S., Vitner, E., Cherry, L., Israeli, O., Beth-Din, A., Paran, N., Israely, T., Yitzaki, S., Levy, H., Weiss, S., 2020. Detection and infectivity potential of severe acute respiratory syndrome coronavirus 2 (SARS-CoV-2) environmental contamination in isolation units and quarantine facilities. Clin. Microbiol. Inf. 26, 1658–1662. https://doi.org/10.1016/j.cmi.2020.09.004.

Biryukov, J., Boydston, J.A., Dunning, R.A., Yeager, J.J., Wood, S., Reese, A.L., Ferris, A., Miller, D., Weaver, W., Zeitouni, N.E., Phillips, A., Freeburger, D., Hooper, I., Ratnesar-Shumate, S., Yolitz, J., Krause, M., Williams, G., Dawson, D.G., Herzog, A.,

Dabisch, P., Wahl, V., Hevey, M.C., Altamura, L.A., 2020. Increasing temperature and relative humidity accelerates inactivation of SARS-CoV2 on surfaces. mSphere 5 e00441-20. https://doi.org/10.1128/mSphere.00441-20.

Bueckert, M., Gupta, R., Gupta, A., Garg, M., Mazumder, A., 2020. Infectivity of SARS-CoV-2 and other coronaviruses on dry surfaces: potential for indirect transmission. Materials 13, 5211. https://doi.org/10.3390/ma13225211.

Centers for Disease Control and Prevention, 2021a. Scientific Brief: SARS-CoV-2 and Potential Airborne Transmission (Accessed June 23, 2021). https://www.cdc.gov/coronavirus/2019-ncov/more/scientific-brief-sars-cov-2.html.

Centers for Disease Control and Prevention, 2021b. COVID-19: Frequently Asked Questions (Accessed June 23, 2021). https://www.cdc.gov/coronavirus/2019-ncov/faq.html#Spread.

Chia, P.Y., Coleman, K.K., Tan, Y.K., Ong, S.W.X., Gum, M., Lau, S.K., Lim, X.F., Lim, A.S., Sutjipto, S., Lee, P.H., Son, T.T., Young, B.E., Milton, D.K., Gray, G.C., Schuster, S., Barkham, T., De, P.P., Vasoo, S., Chan, M., Ang, B.S.P., Tan, B.H., Leo, Y.S., Ng, O.T., Wong, M.S.Y., Marimuthu, K., 2020. Detection of air and surface contamination by SARS-CoV-2 in hospital rooms of infected patients. Nat. Commun. 11, 2800. https://doi.org/10.1038/s41467-020-16670-2.

DeBiasi, R.L., Delaney, M., 2021. Symptomatic and asymptomatic viral shedding in pediatric patients infected with severe acute respiratory syndrome coronavirus 2 (SARS-CoV-2). JAMA Pediatr. 175, 16–18. https://doi.org/10.1001/jamapediatrics.2020.3996.

Ferretti, L., Wymant, C., Kendall, M., Zhao, L., Nurtay, A., Abeler-Dörner, L., Parker, M., Bonsall, D., Fraser, C., 2020. Quantifying SARS-CoV-2 transmission suggests epidemic control with digital contact tracing. Science 368 (6491) eabb6936. https://doi.org/10.1126/science.abb6936.

Gallagher, E.M., Margolin, A.B., 2007. Development of an integrated cell culture–real-time RT-PCR assay for detection of reovirus in biosolids. J. Virol. Methods 139 (2), 195–202. https://doi.org/10.1016/j.jviromet.2006.10.001.

Guo, Z.-D., Wang, Z.-Y., Zhang, S.F., Li, X., Li, L., Li, C., Cui, Y., Fu, R., Dong, Y., Chi, X., Zhang, M., Liu, K., Cao, C., Liu, B., Zhang, K., Gao, Y., Lu, B., Chen, W., 2020. Aerosol and surface distribution of severe acute respiratory syndrome coronavirus 2 in hospital wards, Wuhan, China. Emerg. Infect. Dis. 26, 1583–1591. https://doi.org/10.3201/eid2607.200885.

Harvey, A.P., Fuhrmeister, E.R., Cantrell, M., Pitol, A.K., Swarthout, J.M., Powers, J.E., Nadimpalli, M.L., Julian, T.R., Pickering, A.J., 2021. Longitudinal monitoring of SARS-CoV-2 RNA on high-touch surfaces in a community setting. Environ. Sci. Technol. Lett. 8 (2), 168–175. https://doi.org/10.1021/acs.estlett.0c00875.

He, X., Lau, E.H.Y., Wu, P., Deng, X., Wang, J., Hao, X., Lau, Y.C., Wong, J.Y., Guan, Y., Tan, X., Mo, X., Chen, Y., Liao, B., Chen, W., Hu, F., Zhang, Q., Zhong, M., Wu, Y., Zhao, L., Zhang, F., Cowling, B.J., Li, F., Leung, G.M., 2020. Temporal dynamics in viral shedding and transmissibility of COVID-19. Nat. Med. 26, 1491–1493. https://doi.org/10.1038/s41591-020-1016-z.

Hierholzer, J.C., Killington, R.A., 1996. Virus isolation and quantitation. In: Mahy, B.W.J., Kangro, H.O. (Eds.), Virology Methods Manual. Elsevier Ltd., New York, NY, pp. 25–46. https://doi.org/10.1016/B978-012465330-6/50003-8.

Kampf, G., Bruggemann, Y., Kaba, H.E.J., Steinmann, J., Pfaender, S., Scheithauer, S., Steinmann, E., 2020. Potential sources, modes of transmission and effectiveness of prevention measures against SARS-CoV-2. J. Hosp. Inf. 106, 678–697. https://doi.org/10.1016/j.jhin.2020.09.022.

Kane, S.R., Shah, S.R., Alfaro, T.M., 2019a. Development of a rapid viability polymerase chain reaction method for detection of *Yersinia pestis*. J. Microbiol. Methods 162, 21–27. https://doi.org/10.1016/j.mimet.2019.05.005.

Kane, S.R., Shah, S.R., Alfaro, T.M., 2019b. Rapid viability polymerase chain reaction method for detection of *Francisella tularensis*. J. Microbiol. Methods 166, 105738. https://doi.org/10.1016/j.mimet.2019.105738.

Leibowitz, J., Kaufman, G., Liu, P., 2011. Coronaviruses: propagation, quantification, storage, and construction of recombinant mouse hepatitis virus. Curr. Protoc. Microbiol. 21, 15E.1.1-15E.1.46. https://doi.org/10.1002/9780471729259.mc15e01s21.

Létant, S.E., Murphy, G.A., Alfaro, T.M., Avila, J.R., Kane, S.R., Raber, E., Bunt, T.M., Shah, S.R., 2011. Rapid-viability PCR method for detection of live, virulent *Bacillus anthracis* in environmental samples. Appl. Environ. Microbiol. 77 (18), 6570–6578. https://doi.org/10.1128/AEM.00623-11.

Li, W., Su, Y.Y., Zhi, S.S., Huang, J., Zhuang, C.L., Bai, W.Z., Wan, Y., Meng, X.R., Zhang, L., Zhou, Y.B., Luo, Y.Y., Ge, S.X., Chen, Y.K., May, Y., 2020a. Virus shedding dynamics in asymptomatic and mildly symptomatic patients infected with SARS-CoV-2. Clin. Microbiol. Infect. 26, 1556 e1-1556.e6. https://doi.org/10.1016/j.cmi.2020.07.008.

Li, W., Lin, J., Duan, X., Huang, W., Lu, X., Zhou, J., Zong, Z., 2020b. Asymptomatic COVID-19 patients can contaminate their surroundings: an environment sampling study. mSphere 5 (3) e00442-20. https://doi.org/10.1128/mSphere.00442-20.

Lu, X., Wang, L., Sakthivel, S.K., Whitaker, B., Murray, J., Kamili, S., Lynch, B., Malapati, L., Burke, S.A., Harcourt, J., Tamin, A., Thornburg, N.J., Villanueva, J.M., Lindstrom, S., 2020. US CDC real-time reverse transcription PCR panel for detection of severe acute respiratory syndrome coronavirus 2. Emerg. Infect. Dis. 26 (8), 1654–1665. https://doi.org/10.3201/eid2608.201246.

Luo, L., Liu, D., Zhang, H., Li, Z., Zhen, R., Zhang, X., Xie, H., Song, W., Liu, J., Huang, Q., Liu, J., Yang, X., Chen, Z., Mao, C., 2020. Air and surface contamination in non-health care settings among 641 environmental specimens of 39 COVID-19 cases. PLoS Negl. Trop. Dis. 14 (10), e0008570. https://doi.org/10.1371/journal.pntd.0008570.

Marquès, M., Domingo, J.L., 2021. Contamination of inert surfaces by SARS-CoV-2: persistence, stability and infectivity. A review. Env. Res. 193, 110559 https://doi.org/10.1016/j.envres.2020.110559.

Meyerowitz, E.A., Richterman, A., Gandhi, R.T., Sax, P.E., 2021. Transmission of SARS-CoV-2: a Review of viral, host, and environmental factors. Ann. Intern. Med. 174 (1), 69–79. https://doi.org/10.7326/M20-5008.

Ong, S.W.X., Tan, Y.K., Chia, P.Y., Lee, T.H., Ng, O.T., Wong, M.S.Y., Marimuthu, K., 2020. Air, surface environmental, and personal protective equipment contamination by severe acute respiratory syndrome coronavirus 2 (SARS-CoV-2) from a symptomatic patient. JAMA 323, 1610–1612. https://doi.org/10.1001/jama.2020.3227.

Pastorino, B., Touret, F., Gilles, M., de Lamballerie, X., Charrel, R.N., 2020. Prolonged infectivity of SARS-CoV-2 in fomites. Emerg. Infect. Dis. 26 (9), 2256–2257. https://doi.org/10.3201/eid2609.201788.

Reed, L.J., Muench, H., 1938. A simple method of estimating fifty percent endpoints. Am. J. Epidemiol. 27, 493–497.

Reynolds, K.A., Gerba, C.P., Abbaszadegan, M., Pepper, L.L., 2001. ICC/PCR detection of enteroviruses and hepatitis A virus in environmental samples. Can. J. Microbiol. 47 (2), 153–157. https://doi.org/10.1139/W00-134.

Riddell, S., Goldie, S., Hill, A., Eagles, D., Drew, T.W., 2020. The effect of temperature on persistence of SARS-CoV-2 on common surfaces. Virol. J. 17, 145. https://doi.org/10.1186/s12985-020-01418-7.

Ridinger, D.N., Spendlove, R.S., Barnett, B.B., George, D.B., Roth, J.C., 1982. Evaluation of cell lines and immunofluorescence and plaque assay procedures for quantifying reoviruses in sewage. Appl. Environ. Microbiol. 43 (4), 740–746. https://doi.org/10.1128/AEM.43.4.740-746.1982.

Rigotto, C., Victoria, M., Moresco, V., Kolesnikovas, C.K., Corrêa, A.A., Souza, D.S.M., Miagostovich, M.P., Simões, C.M.O., Baradi, C.R.M., 2010. Assessment of adenovirus, hepatitis A virus and rotavirus presence in environmental samples in Florianopolis, South Brazil. J. Appl. Microbiol. 109 (6), 1979–1987. https://doi.org/10.1111/j.1365-2672.2010.04827.x.

Santarpia, J.L., Rivera, D.N., Herrera, V.L., Morwitzer, M.J., Creager, H.M., Santarpia, G.W., Crown, K.K., Bret-Major, D.M., Schnaubelt, E.R., Broadhurst, M.J., Lawler, J.V., Reid, S.P., Lowe, J.J., 2020. Aerosol and surface contamination of SARS-CoV-2 observed in quarantine and isolation care. Sci. Rep. 10, 1–8. https://doi.org/10.1038/s41598-020-69286-3.

Schmidt, N.J., Ho, H.H., Riggs, J.L., Lennette, E.H., 1978. Comparative sensitivity of various cell culture systems for isolation of viruses from wastewater and fecal samples. Appl. Environ. Microbiol. 36 (3), 480–486. https://doi.org/10.1128/AEM.36.3.480-486.1978.

van Doremalen, N., Bushmaker, T., Morris, D.H., Holbrook, M.G., Gamble, A., Williamson, B.N., Tamin, A., Harcourt, J.L., Thornburg, N.J., Gerber, S.I., Lloyd-Smith, J.O., de Wit, E., Munster, V.J., 2020. Aerosol and surface stability of SARS-CoV-2 as compared with SARS-CoV-1. N. Engl. J. Med. 382 (16), 1564–1567. https://doi.org/10.1056/NEJMc2004973.

van Kampen, J.J.A., van de Vijver, D.A.M.C., Fraaij, P.L.A., Haagmans, B.L., Lamers, M.M., Okba, N., van den Akker, J.P.C., Endeman, H., Gommers, D.A.M.P.J., Cornelissen, J.J., Hoek, R.A.S., van der Eerden, M.M., Hesselink, D.A., Metselaar, H.J., Verbon, A., de Steenwinkel, J.E.M., Aron, G.I., van Gorp, E.C.M., van Boheemen, S., Voermans, J.C., Boucher, C.A.B., Molenkamp, R., Koopmans, M.P.G., Geurtsvankessel, C., van der Eijk, A.A., 2021. Duration and key determinants of infectious virus shedding in hospitalized patients with coronavirus disease-2019 (COVID-19). Nat. Commun. 12, 267. https://doi.org/10.1038/s41467-020-20568-4.

Wei, W.E., Li, Z., Chiew, C.J., Yong, S.E., Toh, M.P., Lee, V.J., 2020. Presymptomatic transmission of SARS-CoV-2 - Singapore, January 23–March 16, 2020. Morb. Mortal. Rep. Surveill. Summ. 69, 411–415. https://doi.org/10.15585/mmwr.mm6914e1.

Wu, S., Wang, Y., Jin, X., Tian, J., Liu, J., Mao, Y., 2020. Environmental contamination by SARS-CoV-2 in a designated hospital for coronavirus disease 2019. Am. J. Infect. Control 48, 910–914. https://doi.org/10.1016/j.ajic.2020.05.003.

Ye, G., Lin, H., Chen, S., Wang, S., Zeng, Z., Wang, W., Zhang, S., Rebmann, T., Li, Y., Pan, Z., Yang, Z., Wang, Y., Wang, F., Qian, Z., Wang, X., 2020. Environmental contamination of SARS-CoV-2 in healthcare premises. J. Infect. 81, e1–e5. https://doi.org/10.1016/j.jinf.2020.04.034.

Zhou, J., Otter, J.A., Price, J.R., Cimpeanu, C., Garcia, D.M., Kinross, J., Boshier, P.R., Mason, S., Bolt, F., Holms, A.H., Barclay, W.S., 2020. Investigating SARS-CoV-2 surface and air contamination in an acute healthcare setting during the peak of the COVID-19 pandemic in London. Clin. Infect. Dis. ciaa905. https://doi.org/10.1093/cid/ciaa905.